Modeling and dynamic analysis of a battlefield water filtration station considering road surface profiles

To Viet Thanh*

Institute of Vehicle and Energy Engineering, Le Quy Don Technical University, 236 Hoang Quoc Viet, Bac Tu Liem, Hanoi, Vietnam.
*Corresponding author: tovietthanh179@gmail.com
Received 27 Jan. 2025; Revised 21 Mar. 2025; Accepted 10 Jun. 2025; Published 25 Jun. 2025.
DOI: https://doi.org/10.54939/1859-1043.j.mst.104.2025.173-181

ABSTRACT

During battlefield operations, mobile water filtration stations are used to supply clean water to military units, one of which is the VFS-2.5 filtration station. When in motion, it tows a trailer carrying a generator and chemical tanks for water filtration. The dynamic model, constructed as a multi-body system, is developed as a planar model with a two-axle truck as the towing vehicle. The study considers the elasticity of the suspension system, tires, and trailer hitch while neglecting the influence of road slope. Based on the dynamic model, the Lagrange equation of the second kind is used to establish the system of differential equations describing the motion of the system. The research model can be utilised to evaluate the stability of the water filtration station, and the aim is to improve the suspension system on the generator trailer to minimise the vibrations of the assembly. This is a highly significant issue in the field of national defence and security.

Keywords: Dynamics; Multi-body system; Water filtration station; Road surface profile; Vehicle vibration; VFS-2.5 model.

1. INTRODUCTION

In the military, water supply operations are a vital task in logistics and technical support. Practically, there are two methods of supplying water during warfare: providing purified water or filtering water from existing sources. For the second method, various filtration stations are mounted on base vehicles, which are trucks that have been operated in the military for several decades. When water tanks affect the vibration dynamics of trucks, some studies have been conducted on vehicle and tractor vibrations. Furthermore, the vibrations of base vehicles have also been studied, taking into account the elasticity of the tires and the suspension system. However, there have been no studies related to dynamic vibrations concerning water filtration stations on military vehicles.

A two-wheel-drive vehicle model moving on a bumpy road with a sinusoidal profile was presented to examine the vehicle's response to the road surface, thereby proposing improvements to the suspension system [1, 2]. In addition, the impact of road surface amplitude on the dynamic parameters of a mobile repair vehicle towing a generator trailer was studied [3]. At a constant speed, a 2D vehicle model with a load distribution along the entire length was used to assess the impact of random road surfaces, stiffness, and the damping coefficient on the vibrations [4]. The analysis of drivetrain parameters along the longitudinal axis and their impact on the vibrations of the vehicle and the driver was examined in [5, 6].

In [7], the study focused on using advanced suspension systems to reduce vibrations during movement as well as improve comfort ability. A similar study, considering the dynamics of a two-wheel-drive vehicle to propose a control strategy aimed at improving ride comfort, was presented in [8]. The work in [9] presents a 3D model with 11 degrees of freedom to examine the impact of vertical vibrations on the driver. The dynamics of four-wheel-drive or five-wheel-drive trucks have also been studied in the references [10, 11]. The impact of vibrations during the movement of trucks is examined on random road surfaces. Some of the aforementioned studies have mentioned

control strategies for the suspension system aimed at reducing vibrations and enhancing comfort for the driver, as discussed in [12-14].

It can be affirmed that there has been no research on the dynamics of a mobile battlefield water filtration station. In this paper, a novel model has been developed and presented the dynamic parameters when the station moves in marching conditions. Moreover, the dynamic vibrations of base vehicles have been evaluated for their impact on the operator and compared with the ISO 2631-1 standard regarding vibrations affecting the operator.

2. DYNAMIC MODEL

The dynamic model based on the VFS-2.5 mobile battlefield water filtration station was made by the Soviet Union, as illustrated in figure 1. The water filtration station consists of two main parts: the base vehicle GAZ-66, which is fitted with the K-66N specialised body carrying equipment for water filtration, disinfection, and the IAPAZ-738 trailer, used to transport the generator, chemical containers, water pumps, and pipes. The IAPAZ-738 trailer is supported by wheels and has no suspension system.

Figure 1. *VFS-2.5 water filtration station in marching condition.*

The dynamic model of the VFS-2.5 water filtration station is displayed in figure 2. The base vehicle has a mass is m_{xcs} (kg) and a moment of inertia at the center of gravity O_1 is J_{xcs} (kg.m^2). The model conducts two motions: vertical displacement y_{xcs} (m) and longitudinal pitching motion φ (°). The front and rear axles have masses of m_{ct} and m_{cs}, respectively, and perform vertical translational motions y_{ct} and y_{cs}. The trailer with a generator has a mass of mrm (kg) and a moment of inertia at the center of mass O_2 is J_{rm} (kg.m^2); it also has two motions: vertical translation y_{rm} (m) and pitch motion in the horizontal direction ψ (°).

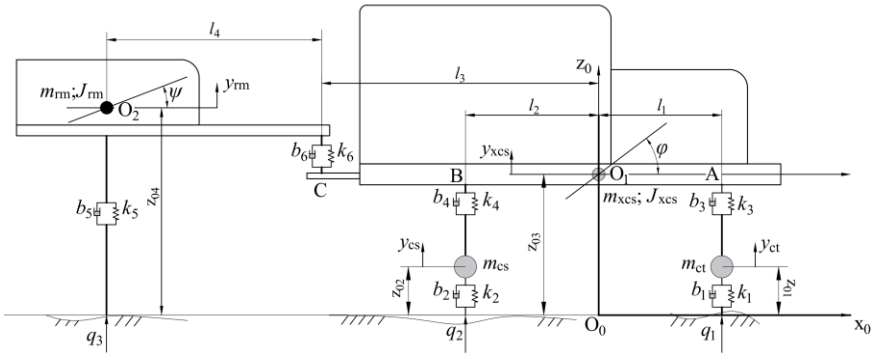

Figure 2. *VFS-2.5 water filtration station moving on the road profile.*

The suspension supports of the base vehicle and trailer are presented by damping coefficients and stiffness values, b_6, k_6; b_1, b_2, b_3, b_4, b_5, they are the damping coefficients of the front and rear tires, the front and rear suspension, and the trailer tires. The stiffness values of the front and rear tires, the front and rear suspension, and the trailer tires are symboled by k_1, k_2, k_3, k_4, k_5. For the

structural parameters: the distance from the center of mass of the base vehicle to the front axle is l_1, whereas the distance from the center of mass of the base vehicle to the rear axle is l_2, the distance from the center of mass of the base vehicle to the suspension support is l_3, the distance from the center of mass of the trailer to the suspension support is l_4. The initial positions z_{01}, z_{02}, z_{03}, z_{04} are vertical distances as drawn in Fig. 2. The functions q_1, q_2, q_3 are the excitations from the ground acting on the respective axles, and these functions depend on time. It can be noted that the effect of road slope on the system is neglected to simplify the simulation.

Generalized coordinates:

It includes 6 parameters:

$$q = \left[q_i\right]^T = \left[y_{ct}\ y_{cs}\ y_{xcs}\ \varphi\ y_{rm}\ \psi\right]^T, \text{ where i = 1÷6.}$$

The dynamic characteristics of the wheeled armored vehicle are represented by a system of five differential equations, which are established based on the Lagrange method of type II, with the equations in the following form:

$$\frac{d}{dt}\left(\frac{T}{\partial \dot{q}_i}\right) - \frac{\partial T}{\partial q_i} + \frac{\partial \Pi}{\partial q_i} + \frac{\partial \Phi}{\partial \dot{q}_i} = Q_i \qquad (i = 1 \div 6) \tag{1}$$

Kinetic energy of the system:

It includes the kinetic energy of the axles, the base vehicle body, and the trailer:

$$T = T_{cx} + T_{xcs} + T_{rm} \tag{2}$$

The kinetic energy of the axles includes the kinetic energy of the first, second, and third axles, respectively:

$$T_{cx} = \frac{1}{2} m_{ct}\left(v^2 + \dot{y}_{ct}^2\right) + \frac{1}{2} m_{cs}\left(v^2 + \dot{y}_{cs}^2\right) \tag{3}$$

The kinetic energy of the base vehicle body is presented by pitching motion φ and vertical oscillation along y_{xcs} :

$$T_{xcs} = \frac{1}{2} m_{xcs}\left(v^2 + \dot{y}_{xcs}^2\right) + \frac{1}{2} J_{xcs}\dot{\varphi}^2 \tag{4}$$

The kinetic energy of the trailer includes pitching motion ψ and the vertical oscillation along y_{rm}:

$$T_{rm} = \frac{1}{2} m_{rm}\left(v^2 + \dot{y}_{rm}^2\right) + \frac{1}{2} J_{rm}\dot{\psi}^2 \tag{5}$$

From Eqs.(2-5), we obtain the kinetic energy of the system, which is determined by the following formula:

$$\begin{aligned} T = {} & \frac{1}{2} m_{ct}\left(v^2 + \dot{y}_{ct}^2\right) + \frac{1}{2} m_{cs}\left(v^2 + \dot{y}_{cs}^2\right) + \frac{1}{2} m_{xcs}\left(v^2 + \dot{y}_{xcs}^2\right) \\ & + \frac{1}{2} m_{rm}\left(v^2 + \dot{y}_{rm}^2\right) + \frac{1}{2} J_{xcs}\dot{\varphi}^2 + \frac{1}{2} J_{rm}\dot{\psi}^2 \end{aligned} \tag{6}$$

Potential energy of the system:

It includes the potential energy of the axle, the potential energy of the base vehicle, and the potential energy of the trailer:

$$\Pi = \Pi_{cx} + \Pi_{xcs} + \Pi_{rm} \tag{7}$$

The potential energy of the axles includes the potential energy of the first and second axles on the GAZ-66 base vehicle and is determined by the equation below:

$$\Pi_{cx} = m_{ct}g\left(z_{01} + y_{ct}\right) + \frac{1}{2}k_1\left(y_{ct} - q_1\right)^2 + m_{cs}g\left(z_{02} + y_{cs}\right) + \frac{1}{2}k_2\left(y_{cs} - q_2\right)^2 \quad (8)$$

The potential energy of the base vehicle is determined by the following formula:

$$\Pi_{xcs} = m_{xcs}g\left(z_{03} + y_{xcs}\right) + \frac{1}{2}k_3\left(y_{xcs} - l_1\varphi - y_{ct}\right)^2 + \frac{1}{2}k_4\left(y_{xcs} + l_1\varphi - y_{cs}\right)^2 \quad (9)$$

The potential energy of the trailer is determined by the following equation:

$$\Pi_{rm} = m_{rm}g\left(z_{04} + y_{rm}\right) + \frac{1}{2}k_5\left(y_{rm} + l_4\psi - y_{xcs} - l_3\varphi\right)^2 \quad (10)$$

From Eqs.(8-10), we obtain the potential energy of the system, which is determined by the following equation:

$$\begin{aligned}\Pi &= m_{ct}g\left(z_{01} + y_{ct}\right) + m_{cs}g\left(z_{02} + y_{cs}\right) + m_{xcs}g\left(z_{03} + y_{xcs}\right) + m_{rm}g\left(z_{04} + y_{rm}\right)\\ &+ \frac{1}{2}k_1\left(y_{ct} - q_1\right)^2 + \frac{1}{2}k_2\left(y_{cs} - q_2\right)^2 + \frac{1}{2}k_3\left(y_{xcs} - l_1\varphi - y_{ct}\right)^2 + \frac{1}{2}k_4\left(y_{xcs} + l_1\varphi - y_{cs}\right)^2\\ &+ \frac{1}{2}k_5\left(y_{rm} - q_3\right)^2 + \frac{1}{2}k_6\left(y_{rm} + l_4\psi - y_{xcs} - l_3\varphi\right)^2\end{aligned} \quad (11)$$

Dissipation function of the system:

It includes the tire dissipation function (ϕ_{lx}), front axle (ϕ_{ct}), rear axle (ϕ_{cs}), and trailer coupling (ϕ_{rm}), and is determined by the following formula:

$$\begin{aligned}\Phi &= \Phi_{lx} + \Phi_{ct} + \Phi_{cs} + \Phi_{rm} = \frac{1}{2}b_1\left(\dot{y}_{ct} - \dot{q}_1\right)^2 + \frac{1}{2}b_2\left(\dot{y}_{cs} - \dot{q}_2\right)^2 + \frac{1}{2}b_3\left(\dot{y}_{xcs} - l_1\dot{\varphi} - \dot{y}_{ct}\right)^2\\ &+ \frac{1}{2}b_4\left(\dot{y}_{xcs} + l_1\dot{\varphi} - \dot{y}_{cs}\right)^2 + \frac{1}{2}b_5\left(\dot{y}_{rm} - \dot{q}_3\right)^2 + \frac{1}{2}b_6\left(\dot{y}_{rm} + l_4\dot{\psi} - \dot{y}_{xcs} - l_3\dot{\varphi}\right)^2\end{aligned} \quad (12)$$

Road bump function:

The road bump function corresponding to the generalized coordinate system $\left[y_{ct}\ y_{cs}\ y_{xcs}\ \varphi\ y_{rm}\ \psi\right]$ is $\left[q_1\ q_2\ 0\ 0\ q_3\ 0\right]$.

According to [3], the road bump profile is described in a sinusoidal form as follows:

$$q(t) = A.\sin\left(\frac{2\pi v_0}{L_0}t\right) \quad (13)$$

Where: v_0 is the vehicle's speed; A and L_0 are the road profile amplitude and the wavelength of the road bump, respectively.

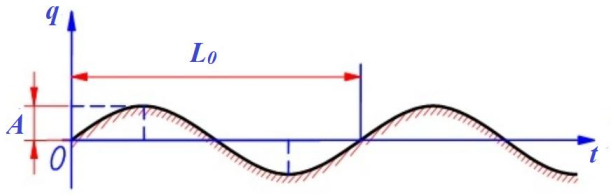

Figure 3. *Road profile.*

In this paper, the vehicle is investigated when moving on a flat road for 5 seconds, then travelling on a deformed road for another 5 seconds, and continuing on a flat road. The delay time of q_2, and q_3 relative to q_1 is determined by the following formula below:

$$t_{try_2} = \frac{l_1 + l_2}{v_0}; t_{try_3} = \frac{l_1 + l_3 + l_4}{v_0}$$

Therefore, the bump functions q_1, q_2, and q_3 are defined as follows:

$$q_1 = \begin{cases} A.\sin\left(\dfrac{2\pi v_0}{L_0}t\right) & 5 < t \le 10 \\ 0 & 0 \le t \le 5; t > 10 \end{cases} \tag{14}$$

$$q_2 = \begin{cases} A.\sin\left(\dfrac{2\pi v_0}{L_0}t\right) & 5 + t_{try2} < t \le 10 + t_{try2} \\ 0 & 0 \le t \le 5 + t_{try2}; t > 10 + t_{try2} \end{cases} \tag{15}$$

$$q_3 = \begin{cases} A.\sin\left(\dfrac{2\pi v_0}{L_0}t\right) & 5 + t_{try3} < t \le 10 + t_{try3} \\ 0 & 0 \le t \le 5 + t_{try3}; t > 10 + t_{try3} \end{cases} \tag{16}$$

Substituting the expressions for kinetic energy, potential energy, dissipation function, and generalized forces into formula (1), we obtain a set of differential equations describing the motion of the system:

$$m_{ct}\ddot{y}_{ct} + (b_1 + b_3)\dot{y}_{ct} - b_3\dot{y}_{xcs} + b_3 l_1\dot{\varphi} + (k_1 + k_3)y_{ct} - k_3 y_{xcs} + k_3 l_1\varphi + m_{ct}g = k_1 q_1 + b_1\dot{q}_1 \tag{17}$$

$$m_{cs}\ddot{y}_{cs} + (b_2 + b_4)\dot{y}_{cs} - b_4\dot{y}_{xcs} - b_4 l_1\dot{\varphi} + (k_2 + k_4)y_{cs} - k_4 y_{xcs} - k_4 l_1\varphi + m_{cs}g = k_2 q_2 + b_2\dot{q}_2 \tag{18}$$

$$\begin{aligned} &m_{xcs}\ddot{y}_{xcs} - b_3\dot{y}_{ct} - b_4\dot{y}_{cs} + (b_3 + b_4)\dot{y}_{xcs} - (b_3 l_1 - b_4 l_1 - b_6 l_3)\dot{\varphi} - b_6\dot{y}_{rm} - b_6 l_4\dot{\psi} - k_3 y_{ct} + k_4 y_{cs} \\ &+ (k_3 + k_4)y_{xcs} - (k_3 l_1 - k_4 l_1 - k_6 l_3)\varphi - k_6 y_{rm} + k_6 l_4\psi = 0 \end{aligned} \tag{19}$$

$$\begin{aligned} &J_{xcs}\ddot{\varphi} + b_3 l_1\dot{y}_{ct} + b_4 l_1\dot{y}_{cs} - (b_3 l_1 - b_4 l_1 - b_6 l_3)\dot{y}_{xcs} + (b_3 l_1^2 + b_4 l_1^2 + b_6 l_3^2)\dot{\varphi} - b_6 l_3 l_4\dot{\psi} + k_3 l_1 y_{ct} \\ &- k_4 l_1 y_{cs} - (k_3 l_1 - k_4 l_1 - k_6 l_3)y_{xcs} + (k_3 l_1^2 + k_4 l_1^2 + k_6 l_3^2)\varphi - k_6 l_3 l_4\psi = 0 \end{aligned} \tag{20}$$

$$\begin{aligned} &m_{rm}\ddot{y}_{rm} - b_6\dot{y}_{xcs} - b_6 l_3\dot{\varphi} + (b_5 + b_6)\dot{y}_{rm} + b_6 l_4\dot{\psi} - k_6 y_{xcs} - k_6 l_3\varphi \\ &+ (k_5 + k_6)y_{rm} + k_6 l_4\psi = k_6 q_3 + b_6\dot{q}_3 \end{aligned} \tag{21}$$

$$J_{rm}\ddot{\psi} - b_6 l_4\dot{y}_{xcs} - b_6 l_3 l_4\dot{\varphi} + b_6 l_4\dot{y}_{rm} + b_6 l_4^2\dot{\psi} - k_6 l_4 y_{xcs} - k_6 l_3 l_4\varphi + k_6 l_4 y_{rm} + k_6 l_4^2\psi = 0 \tag{22}$$

3. RESULTS AND DISCUSSION

3.1. Input data

The initial condition:

$$[y_{ct}\ y_{cs}\ y_{xcs}\ \varphi\ y_{rm}\ \psi] = [0\ 0\ 0\ 0\ 0\ 0]$$

The bump function of road profile q1 is plotted by a dotted back curve, while road profile q2 is shown by a dashed green curve, and road profile q3 is described by a solid red curve.

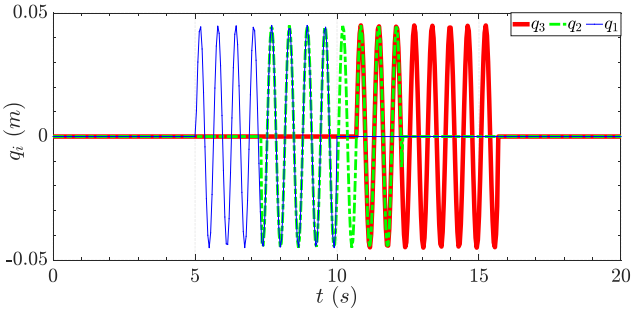

Figure 4. *Sinusoidal road roughness profile.*

Table 1. *Input parameters [15].*

Parameters	Value	Parameters	Value	Parameters	Value
k_1	430000 (N/m)	b_3	24000 (Ns/m)	J_{xcs}	8879 (kg.m^2)
k_2	430000 (N/m)	b_4	11500 (Ns/m)	J_{rm}	352 (kg.m^2)
k_3	100000 (N/m)	b_5	500 (Ns/m)	m_{ct}	520(kg)
k_4	106000 (N/m)	b_6	500 (Ns/m)	m_{cs}	480(kg)
k_5	430000 (N/m)	l_1	2,25 (m)	m_{xcs}	6000 (kg)
k_6	4.10^5 (N/m)	l_2	1,07 (m)	m_{rm}	2000(kg)
b_1	500 (Ns/m)	l_3	2,37 (m)	L_0	0,6 (m)
b_2	500 (Ns/m)	l_4	2,06 (m)	v_0	1,2 m/s

3.2. Simulation results and discussion

Using the input parameters in table 1, the system of differential equations from (16) to (21) is solved by the **ode45** method in Matlab, the study obtains the displacements and pitch motions, which are depicted in figures 5, 6, 7, 8, and 9 below:

- Results of axle displacement (Fig. 5a and Fig. 5b): The vibration patterns and graphs for both axles are quite similar. During the first 5 seconds, as the system shifts from a static to a dynamic state, the oscillation amplitude of both axles increases gradually. Notably, when the rear axle encounters the bump, the oscillation amplitude rises sharply, reaching a peak of approximately 4.2 cm for the front axle and 4 cm for the rear axle. Once the vehicle moves off the bumpy road and onto a smooth surface, the oscillations of the axles progressively decrease due to the damping effect of the tires.

- Results of base vehicle displacement.

+ Vertical displacement of the base vehicle (Fig. 5c): The vertical vibration of the base vehicle also follows a sinusoidal pattern. As the rear axle crosses the bump, the oscillation amplitude increases sharply, reaching a peak of approximately 5 cm at 15 seconds. Once the vehicle moves off the bumpy road and onto a smooth surface, the oscillation of the base vehicle body gradually diminishes due to the damping effect of the tires.

+ Pitch angle of the base vehicle (Fig. 5d): For pitch dynamics, the pitch motion of the base vehicle has a sinusoidal shape. After the transient period, the vibration amplitude increases notably, reaching a peak of around 1.5°. The practical vehicle has a pitch angle range from 0° to 7°. Therefore, the pitch motion of the base vehicle still ensures ride comfort. Once the vehicle passes over the bumpy road and moves onto a flat surface, the pitch motion of the base vehicle gradually decreases, influenced by the damping effect of the tires.

- Results of trailer displacement:

+ Trailer's displacement (Fig. 5e): The vertical oscillation of the trailer follows a sinusoidal pattern. The vibrating amplitude of the trailer gradually increases after the initial period; the oscillation amplitude increases sharply and reaches a maximum amplitude of around 4 cm. However, the absolute displacement amplitude is only 2 cm on the other side. After passing over the bumpy road and moving onto a flat surface, under the damping effect of the tires, the trailer oscillates following a decreasing pattern.

+ Pitch angle of the trailer (Fig. 5f): The pitch angle of the trailer vibrates following a sinusoidal pattern. In the first 5 seconds, the system transitions from a static to a dynamic state, the amplitude of the base vehicle's oscillation gradually increases; particularly during the delay when the trailer enters the bump, the amplitude of oscillation increases significantly and reaches a maximum amplitude of about 1.3°. The real-world vehicle has a pitch angle ranging from 0° to 7°, it can be

concluded that the trailer's pitch motion stays within the ride comfort limits. After passing over the bumpy road and moving onto a flat surface, under the damping effect of the tires, the pitch angle of the base vehicle gradually decreases. This reduction in pitch motion after 17 seconds provides better ride comfort.

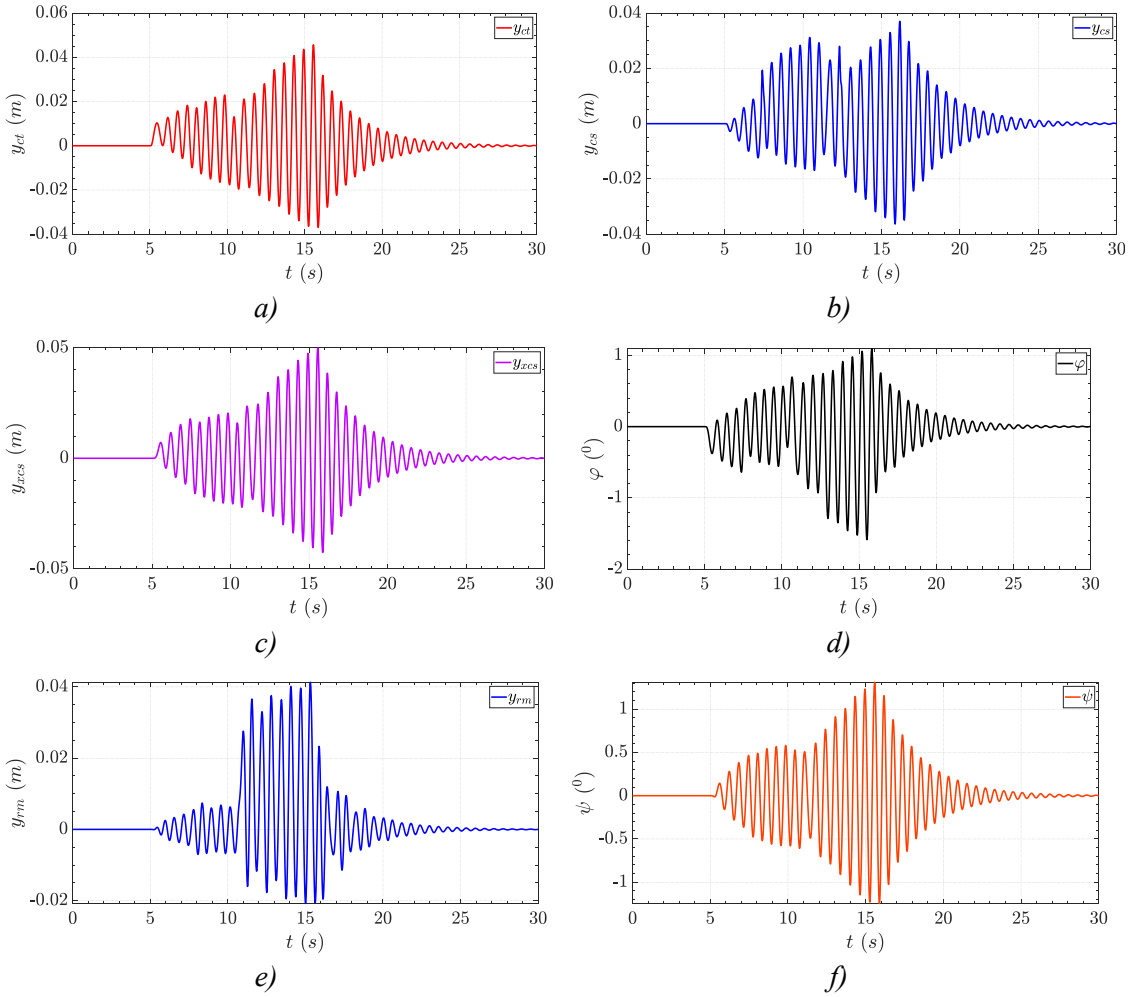

Figure 5. *Displacement graph of the bodies*

a) Front axle displacement; b) Rear axle displacement;

c) Vertical displacement of the base vehicle; d) Pitch angle of the base vehicle;

e) Vertical displacement of the trailer; f) Pitch angle of the trailer

- Evaluation of vibrations impacting the operator: The acceleration in the vertical direction of the base vehicle body also vibrates following a sinusoidal pattern. During the first 5 seconds, the base vehicle's acceleration steadily rises; especially after a delay when the rear axle enters the bump, the acceleration increases significantly and reaches a maximum amplitude of about 0.3 (m/s²). After passing over the bumpy road and moving onto a flat surface, under the damping effect of the tires, the axle acceleration reduces gradually. This is entirely consistent with real-world behavior. Based on the surveyed acceleration results and according to the ISO 2631-1 standard on vibrations [16], the acceleration impacting the operator remains below 0.5 (m/s²). Therefore, moving on a bumpy road with a profile of 0.045 (m) ensures a comfortable ride for the operator.

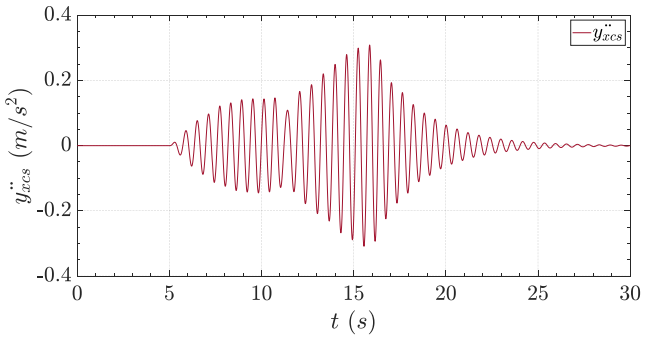

Figure 6. *Acceleration of the base vehicle.*

4. CONCLUSIONS

This paper has developed a dynamic model of the mobile water filtration station, taking into account a sinusoidal road profile. Based on the dynamic model, the vertical displacement of the axles and the pitch angles of the base vehicle body, as well as the trailer, were investigated. Furthermore, the dynamic vibrations impacting the driver during movement were evaluated. The survey results demonstrate that the maximum displacement amplitude of the front axle is 4.2 cm, the rear axle is 4 cm, the base vehicle body is 5 cm, the pitch angle of the base vehicle is 1.5°, the trailer displacement is 4 cm, and the trailer pitch angle is 1.3°. Correspondingly, the maximum acceleration of the base vehicle body is 0.3 (m/s²). Compared with the ISO 2631-1 standard on vibrations affecting the operator, it can be concluded that when the water filtration station moves on a sinusoidal road surface with an amplitude of 0.045 m, it ensures a comfortable ride during operation. The results of the paper provide the basis for evaluating the stability of the water filtration station and aim to improve the suspension system on the generator trailer to minimize the dynamic vibrations.

REFERENCES

[1]. M. Boreiry, S. Ebrahimi-Nejad and J. Marzbanrad, "*Sensitivity analysis of chaotic vibrations of a full vehicle model with magnetorheological damper*", Chaos. Solitons and Fractals, vol. 127, pp. 428-442, (2019). https://doi.org/10.1016/j.chaos.2019.07.005.

[2]. Q. Zhu and M. Ishitobi, *"Chaotic vibration of a nonlinear full-vehicle model"*, International Journal of Solids and Structures, vol. 43, no. 3-4, pp. 747–759, (2006), https://doi.org/10.1016/j.ijsolstr.2005.06.070.

[3]. Nguyen Minh Kha, Le Van Duong, Tran Duc Thang, "*Study on the impact of ground profile on the vibrations of military mobile repair vehicles*", Vietnam mechanical Journal, No. 11, pp.154-159, (2024).

[4]. D. W. Park, A. T. Papagiannakis and I. T. Kim, *"Analysis of Dynamic Vehicle Loads using Vehicle Pavement Interaction Model"*, KSCE Journal of Civil Engineering, vol 18, no. 7, pp.2085-2092, (2014). https://doi.org/10.1007/s12205-014-0602-3.

[5]. D. Miroslav, B. S. Zeljko and M. M. Danijela, *"Impact of truck'spower trainlayout on driver's foreand-aft vibration loads*", Journal of Mechanical Engineering and Modern Technology, vol. 1, no. 1, pp. 37-51, (2018). http://www.jmemt.jarap.org

[6]. L. E. Davis and J. M. Bunker, *"Dynamic load sharing for heavy vehicles a new metric"*, Road and Transport Research, vol. 18, no. 4, pp. 23-37, (2009). https://www.researchgate.net/publication/43206184.

[7]. Z. Jie, D. Yuanwang, Z. Nong and Z. Bangji, *"Vibration Performance Analysis of a Mining Vehicle with Bounce and Pitch Tuned Hydraulically Interconnected Suspension"*, Chinese Journal of Mechanical Engineering, vol. 32, no. 5, (2019). https://doi.org/10.1186/s10033-019-0315-0.

[8]. T. Attia, K. G. Vamvoudakis, K. Kochersberger, J. Bird and T. Furukawa, *"Simultaneous dynamic system estimation and optimal control of vehicle active suspension"*, Vehicle System Dynamics, vol. 57, no. 10, pp. 1467–1493, (2019). https://doi.org/10.1080/00423114.2018.1521000

[9]. S. Aziz and A. Z. Yunus, *"Analysis of the vertical vibration effects on ride comfort of vehicle driver"*, Journal of Vibroengineering, vol. 14, no. 2, pp. 559-571, (2012). https://www.extrica.com/article/10613

[10]. T. T. Hung, D. N. Khanh and L. V. Quynh, *"Analyzing the effect of vehicle speed and class of random road profile on a 4-axle truck vehicle vibration"*, ARPN Journal of Engineering and Applied Sciences, vol. 18, no. 9, pp. 1052-1057, (2023). https://www.arpnjournals.com/jeas/volume_09_2023.htm

[11]. L. V. Quynh, J. Zhang, X. Liu and Y. Wang, *"Nonlinear dynamic analysis of interaction between vehicle and road surfaces for 5-axle heavy truck"*, Journal of Southeast University, vol. 27, no. 4, pp. 405-409, (2011). https://doi.org/10.3969/j.issn.10037985.2011.04.012.

[12]. M. P. Nagarkar, G. J. Vikhe, K. R. Borole and V. M. Nandedkar, *"Active Control of Quarter Car Suspension System using Linear Quadratic Regulator"*, Int. J. Automot. Mech. Eng, vol. 3, 364-372, (2022). https://doi.org/10.15282/ijame.3.2011.11.0030.

[13]. V. M. Barethiye, G. Pohit and A. Mitra, *"Analysis of a quarter car suspension system based on nonlinear shock absorber damping models"*, Int. J. Automot. Mech. Eng., vol. 14, no. 3, pp. 4401-4418, (2022). https://doi.org/10.15282/ijame.14.3.2017.2.0349.

[14]. A. Ferhath and K. Kasi, *"A Review on Various Control Strategies and Algorithms in Vehicle Suspension Systems"*, Int. J. Automot. Mech. Eng., vol. 20, no. 3, pp. 10720-10735, (2023). https://doi.org/10.15282/ijame.20.3.2023.14.0828.

[15]. Н.П. Агарков, С.П. Александрович, С.И. Блажко, В.И. Булах*,...."Инженерные войска вооруженных сил российской федерации"*, Для служебного пользования, Экз. № 1, Каталог средства инженерного вооружения, Книга 2, Москва.

[16]. International Standard, ISO 2631-1, "*Mechanical vibration and shock - Evaluation of human exposure to whole-body vibration*", (2010).

TÓM TẮT

Mô hình hóa và phân tích động lực học trạm lọc nước dã chiến khi di chuyển có xét đến biên dạng mặt đường

Trong quá trình tác chiến trên chiến trường, trạm lọc nước dã chiến được sử dụng để cung cấp nước sạch cho các đơn vị một trong số đó là trạm lọc nước VFS-2,5. Khi di chuyển, chúng kéo theo rơ-mooc chở máy phát điện và thùng hóa chất phía sau để lọc nước. Mô hình động lực học ở dạng cơ hệ nhiều vật được xây dựng là mô hình phẳng với xe kéo là xe tải hai cầu. Mô hình nghiên cứu xem xét đến sự đàn hồi của hệ thống treo, lốp xe, khớp nối rơ-mooc và bỏ quả ảnh hưởng của độ dốc. Trên cơ sở mô hình động lực học, phương trình La-grăng loại II được sử dụng để xây dựng hệ phương trình vi phân mô tả chuyển động của cơ hệ. Mô hình nghiên cứu có thể được sử dụng để đánh giá độ ổn định của trạm lọc nước và hướng đến cải tiến hệ thống treo trên rơ-mooc kéo máy phát điện nhằm giảm thiểu dao động của tổ hợp. Đây là vấn đề rất có ý nghĩa trong lĩnh vực an ninh quốc phòng.

Từ khoá: Động lực học; Hệ nhiều vật; Trạm lọc nước; Biên dạng mặt đường; Dao động phương tiện cơ giới; Mô hình VFS 2.5.